land

MDPI

Article

Characteristics of Soil Erodibility K Value and Its Influencing Factors in the Changyan Watershed, Southwest Hubei, China

Xiaofang Huang [1], Lirong Lin [2,3,4,*], Shuwen Ding [1,3,4], Zhengchao Tian [2,3,4], Xinyuan Zhu [1], Keren Wu [5] and Yuanzhe Zhao [2]

[1] Department of Ecology, College of Resources and Environment, Huazhong Agricultural University, Wuhan 430070, China; xiaofang2019@webmail.hzau.edu.cn (X.H.); dingshuwen@mail.hzau.edu.cn (S.D.); zhu1245065366@163.com (X.Z.)

[2] Department of Soil and Plant Nutrition, College of Resources and Environment, Huazhong Agricultural University, Wuhan 430070, China; tianzhengchao@mail.hzau.edu.cn (Z.T.); Z_yz@webmail.hzau.edu.cn (Y.Z.)

[3] Key Laboratory of Arable Land Conservation (Middle and Lower Reaches of Yangtze River), Ministry of Agriculture and Rural Affairs, Wuhan 430070, China

[4] State Environmental Protection Key Laboratory of Soil Health and Green Remediation, Wuhan 430070, China

[5] Department of Resource and Environmental Information Engineering, College of Resources and Environment, Huazhong Agricultural University, Wuhan 430070, China; roselsy@126.com

* Correspondence: lrlin@mail.hzau.edu.cn; Tel.: +86-132-7708-7428

Abstract: Soil erodibility K factor is an important parameter for evaluating soil erosion vulnerability and is required for soil erosion prediction models. It is also necessary for soil and water conservation management. In this study, we investigated the spatial variability characteristics of soil erodibility K factor in a watershed (Changyan watershed with an area of 8.59 km^2) of Enshi, southwest of Hubei, China, and evaluated its influencing factors. The soil K values were determined by the EPIC model using the soil survey data across the watershed. Spatial K value prediction was conducted by regression-kriging using geographic data. We also assessed the effects of soil type, land use, and topography on the K value variations. The results showed that soil erodibility K values varied between 0.039–0.052 t·hm^2·h/(hm^2·MJ·mm) in the watershed with a block-like structure of spatial distribution. The soil erodibility, soil texture, and organic matter content all showed positive spatial autocorrelation. The spatial variability of the K value was related to soil type, land use, and topography. The calcareous soil had the greatest K value on average, followed by the paddy soil, the yellow-brown soil (an alfisol), the purple soil (an inceptisol), and the fluvo-aquic soil (an entisol). The soil K factor showed a negative correlation with the sand content but was positively related to soil silt and clay contents. Forest soils had a greater ability to resist to erosion compared to the cultivated soils. The soil K values increased with increasing slope and showed a decreasing trend with increasing altitude.

Keywords: soil erodibility; EPIC model; spatial variability; watershed

1. Introduction

Erosion can directly or indirectly cause soil quality decline, land degradation, soil resource loss of arable land and even result in serious natural disasters [1–3]. Among the many factors affecting soil erosion, the inherent resistance of soil to erosional processes, which is usually expressed as the soil erodibility K factor, is an important parameter in evaluating and predicting soil erosion intensity [4,5]. Soil erodibility K factor is also generally considered as the susceptibility of soil to erosional processes such as rain splash, surface runoff, and interflow, and it is the basis for quantifying the effects of soil properties on erosion [6–8].

At present, plenty of researchers have investigated the effects of soil and environmental properties on erodibility, compared the performance of different soil K factor estimation methods, and evaluated spatial variability characteristics and influencing factors of the

K value in the regions at different scales [9–12]. Zhang et al. (2009) compared five K value prediction methods, including the EPIC model and the Torri model, to evaluate the uncertainty of soil K prediction in subtropical regions [13]. Godoi et al. (2021) showed that the USLE model could estimate the K factor of Brazil soils more accurately than did the EPIC model [14]. Madenoglu et al. (2020) assessed the spatial uncertainty of the soil erodibility factor by using the kriging method and direct sequential simulation method for the Ankara Sakarya Basin in Turkey [15]. Martínez-Murillo et al. (2020) verified the validity of the RUSLE K factor by the stability of agglomerates in the Mediterranean mountains of southern Spain [16]. In addition, these methods did not consider the spatial autocorrelation of soil erodibility K values and influencing factors in small watersheds, resulting in the loss of information on the degree of spatial aggregation.

Spatial autocorrelation analysis is a method to analyze the correlation and significance of spatial data and combining it with soil erodibility evaluation can better reveal the spatial clustering characteristics of regional soil erodibility [17,18]. The Moran index is a commonly used spatial autocorrelation metric that can be used to describe the spatial characteristics of variables [19,20]. Compared with Lin's consistent correlation coefficient, which is commonly used to compare two measurements of the same variable [21], the regression modeling method is more capable of rapidly modeling the relationship in the independent and dependent variables and is especially effective for small datasets and simple relationships. For example, Zhao et al. (2020) combined soil apparent electrical conductivity with CEC at different depths by a linear regression (LR) model [22], and Ma et al. (2015) performed a regression analysis between soil erodibility and soil total N and total P loss in northern China [23]. Thus, an effective combination of spatial autocorrelation analysis and linear regression may be helpful to study soil erodibility K values.

Future research on the soil erodibility K factor is required for further understanding soil erosion mechanisms, the quantification of erosion processes at various scales and in areas with complicated soil types [24–26]. The southwest region of Hubei province is located at the eastern edge of the Yunnan-Guizhou Plateau of China, with numbers of deep river valleys, a fragile terrain, and a complex and variable environment, and it suffers from serious soil erosion [27]. According to the data of the 2020 Hubei bulletin of soil and water conservation, the soil erosion region covered an area of 7309.51 km^2, accounting for 29.64% of the total land area of this region [28].

Recently, several studies have reported the characteristics of soil erosion in the rocky desertification regions of southwest China, the effect of hydropower projects on soil and water conservation in Hubei province, spatial and temporal variation of the soil erosion patterns in the forest and agricultural ecosystems, and the performance of the forest rehabilitation from slope agriculture project on soil and water conservation [29–32]. However, there is a lack of studies in soil erosion mechanisms and spatial erodibility variations related to the southwest of Hubei province which are important for soil erosion intensity prediction and soil and water conservation management in this region.

In this study, we investigated the soil erodibility K factor variations in a typical small watershed (Changyan watershed) in Enshi, southwest of Hubei province. A soil survey was conducted across the watershed and the EPIC model was used to predict the soil K values. The geographic data were interpolated via the regression-kriging method for the assessment of the spatial variability of the K factor. The results from this study can be used for the soil erosion intensity prediction of the southwest region of Hubei province and regions with similar topography and environment conditions and can be useful for local soil and water management.

2. Materials and Methods

2.1. Study Area

The Changyan watershed (109°29′23.08″ E~109°33′20.39″ E, 30°11′25.54″ N~30°15′22.85″ N) is in the mountainous area of the south-central Enshi Prefecture, Hubei province, China (Figure 1). It is a catchment with total area of 8.59 km^2 of a first-class tributary of

Qingjiang River. The region has a typical subtropical monsoon climate with an annual average temperature of 18.1 °C, an extreme maximum temperature of 41.2 °C, an annual average rainfall of 1470.2 mm and an annual average relative humidity of 81%. The main soil types in the watershed include yellow-brown soil (an alfisol), paddy soil, calcareous soil, purple soil (an inceptisol), and fluvo-aquic soil (an entisol), with yellow-brown soil accounting for 59.37 percent of the watershed area. Part of the watershed is covered by bare rocks including limestone, shale, sandstone, and siltstone. The watershed has a fragile terrain topography surrounded by steep mountains and hills. The high-altitude part of the catchment is located at the northeast and the low-altitude part is in the southwest and the elevation ranges from 413 to 919 m. The slope land was mainly used as forest, orchard, and cultivated field for planting *Pinus massoniana*, *Cunninghamia lanceolate*, *Cinnamomum camphora*, *Osmanthus fragrans*, *Citrus reticulata*, *Camellia sinensis*, *Zea mays*, and *Oryza sativa*.
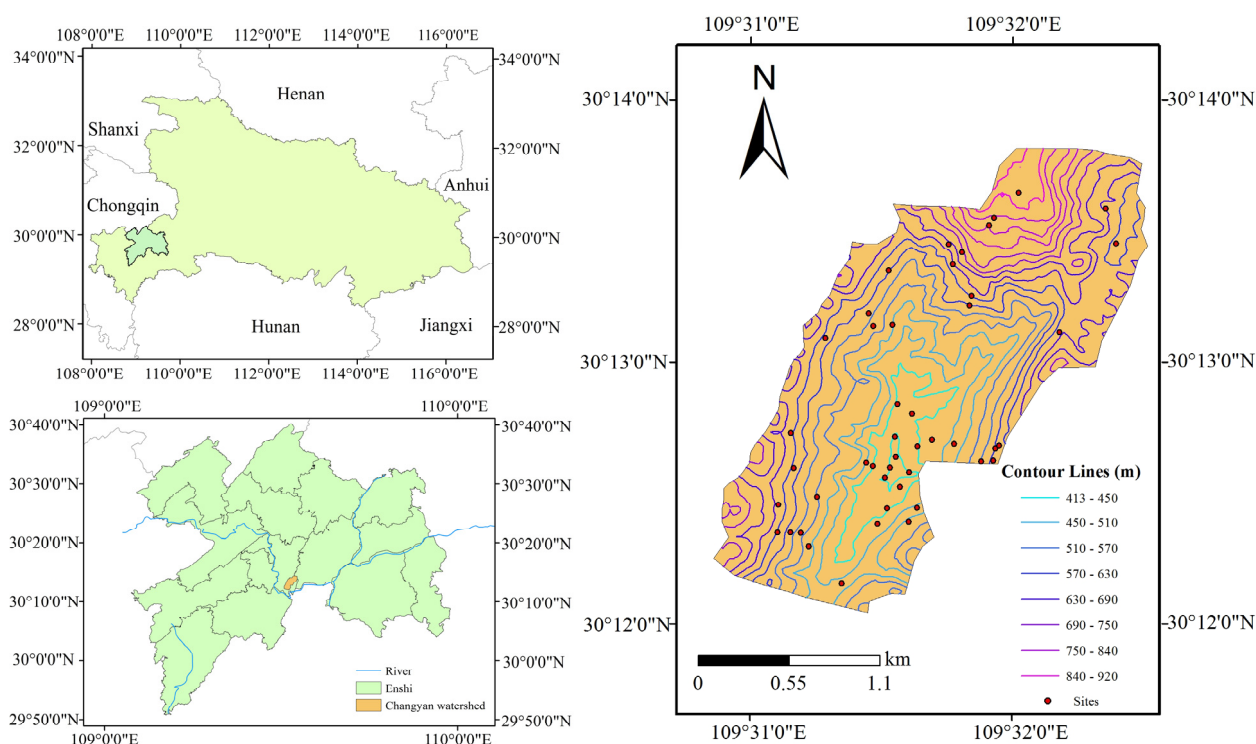

Figure 1. Location, topographic contour map, and sampling sites of the study area.

2.2. Data Collection and Interpretation

The DEM data of the watershed were obtained from the geospatial data cloud (https://www.gscloud.cn/, accessed on 10 October 2020). The land use classification result was derived from sentinel-2 image with a spatial resolution of 12.5 m. The soil distribution information was initially extracted from the 1:250,000 soil map of Hubei Province. To further improve the spatial resolution of the soil and determine the land use type, we conducted a field survey across the watershed and classified the soil type at a high spatial resolution using the in situ measurement with reference to the Chinese soil taxonomy [33]. The field survey map unit and soil sampling points were selected by integrating the information of previous soil map, land use information, DEM data, regional soil erosion characteristics, and other related information of the watershed (Table 1). The field survey was carried out in November 2020, and samples from the surface soil layer (0–10 cm) were collected. In the lab, gravels and organic debris, such as roots in the soil, were removed. After that, samples were air-dried and finely ground to pass through a 2 mm sieve for use. Soil physical and chemical properties such as pH, soil texture, and organic carbon content were determined by the pH meter method, the pipette method, and the Dichromate method [34], respectively,

and the soil organic matter content was obtained by multiplying the soil organic carbon concentration by 1.724 [35].

Table 1. Basic information on sampling sites.

Sampling Points	Slope Direction	Slope (°)	Altitude(m)	Land-Use Type	Type of Soil	pH
C1	W290	45	423	Orchard—*Citrus reticulata*	Paddy soil	6.69
C2	W265	35	417	Forest—*Osmanthus fragrans*	Purple soil	8.18
C3	N340	47	452	Orchard—*Citrus reticulata*	Yellow-brown loam	6.25
C4	N350	24	483	Forest—*Pinus massoniana*	Yellow-brown loam	5.74
C5	W282	39	373	Forest—*Pinus massoniana*	Yellow-brown loam	5.77
C6	W293	41	427	Cultivate land—*Cucurbita* moschata	Fluvo-auic soil	8.34
C7	NW310	29	392	Orchard—*Citrus reticulata*	Paddy soil	8.42
C8	SE124	35	405	Forest—*Osmanthus fragrans*	Purple soil	8.2
C9	SE145	24	389	Orchard—*Citrus reticulata*	Calcareous soil	6.72
C10	SE131	35	456	Orchard—*Citrus reticulata*	Calcareous soil	6.37
C11	SE116	21	503	Orchard—*Citrus reticulata*	Yellow-brown loam	6.43
C12	E104	25	608	Orchard—*Citrus reticulata*	Paddy soil	8.44
C13	W269	10	416	Orchard—*Citrus reticulata*	Yellow-brown loam	5.74
C14	W289	13	465	Cultivated—*Zea mays*	Yellow-brown loam	6.27
C15	W292	43	556	Forest—*Cunninghamia lanceolata*	Yellow-brown loam	7.42
C16	W293	26	594	Forest—*Pinus massoniana*	Yellow-brown loam	5
C17	NE33	25	860	Forest—*Pinus massoniana*	Yellow-brown loam	4.88
C18	SW233	43	829	Forest—*Pinus massoniana*	Yellow-brown loam	4.6
C19	W244	37	789	Forest—*Pinus massoniana*	Purple soil	6.37
C20	W264	35	683	Cultivated land—*Ipomoea batatas*	Fluvo-auic soil	7.24
C21	SW235	32	657	Cultivated land—*Zea mays*	Purple soil	7.46
C22	SW223	28	644	Orchard—*Citrus reticulata*	Yellow-brown loam	4.97
C23	S160	20	545	Forest—*Cunninghamia lanceolata*	Yellow-brown loam	6.61
C24	SE121	26	533	Forest—*Cunninghamia lanceolata*	Yellow-brown loam	6.7
C25	SE116	30	480	Orchard—*Citrus reticulata*	Yellow-brown loam	5.75
C26	SE115	17	415	Orchard—*Citrus reticulata*	Paddy soil	7.67
C27	S165	11	387	Grassland—*Pteridophyta*	Paddy soil	8.09
C28	N350	28	411	Forest—*Cinnamomum camphora*	Yellow-brown loam	8.02
C29	N290	27	420	Orchard—*Citrus reticulata*	Yellow-brown loam	7.37
C30	N14	25	476	Orchard—*Citrus reticulata*	Yellow-brown loam	7.01
C31	E107	33	592	Forest—*Osmanthus fragrans*	Yellow-brown loam	7.18
C32	SE133	32	549	Orchard—*Citrus reticulata*	Yellow-brown loam	7.26
C33	SE133	27	521	Forest—*Cinnamomum camphora*	Yellow-brown loam	7.2
C34	E76	36	486	Orchard—*Citrus reticulata*	Yellow-brown loam	7.16
C35	SE145	20	593	Forest—*Berberis thunbergii* 'Atropurpurea'	Yellow-brown loam	6.53
C36	SE116	22	605	Forest—*Cinnamomum camphora*	Yellow-brown loam	6.48
C37	SE129	26	587	Orchard—*Citrus reticulata*	Paddy soil	6.79
C38	SE141	29	579	Orchard—*Citrus reticulata*	Purple soil	7.06
C39	SW209	20	582	Forest—*Pinus massoniana*	Purple soil	7.05
C40	W257	19	623	Grassland—*Pteridophyta*	Yellow-brown loam	7.27
C41	E109	20	609	Cultivated—*Oryza sativa*	Paddy soil	6.71
C42	W263	17	587	Forest—*Cinnamomum camphora*	Yellow-brown loam	6.7
C43	W274	20	624	Orchard—*Citrus reticulata*	Yellow-brown loam	6.74
C44	W281	18	587	Forest—*Pinus massoniana*	Yellow-brown loam	6.44
C45	W279	20	588	Forest—*Cinnamomum camphora*	Purple soil	5.49
C46	E72	28	424	Forest—*Cinnamomum camphora*	Yellow-brown loam	7.08

2.3. Methods

2.3.1. Soil Erodibility K Value Prediction

In this study, we estimated the soil erodibility K values from the soil physical and chemical properties using the EPIC model as follows [36]:

$$
\begin{aligned}
\text{K} = &\left\{ 0.2 + 0.3 \times \exp\left[-0.0256 \times \text{SAN} \times \left(1 - \tfrac{\text{SIL}}{100} \right) \right] \right\} \times \left(\tfrac{\text{SIL}}{\text{CLA+SIL}} \right)^{0.3} \times \\
&\left[1.0 - \tfrac{0.25 \times \text{C}}{\text{C} + \exp(3.72 - 2.95 \times \text{C})} \right] \times \\
&\left\{ 1.0 - \tfrac{0.7 \times \text{SN1}}{\text{SN1} + \exp(-5.51 + 22.9 \times \text{SN1})} \right\}
\end{aligned}
\tag{1}
$$

where SAN is the soil sand content (%); SIL is the silt content (%); CLA is the clay content (%), SN1 = 1-SAN/100; and C is the organic carbon content (%). The K values obtained from the above model were further divided by 7.593 to convert soil erodibility into the SI unit of $t \cdot hm^2 \cdot h/(hm^2 \cdot MJ \cdot mm)$.

2.3.2. Spatial Autocorrelation Analysis

The Moran's I index can be used to reveal the similarity or correlation between the spatial reference unit and its neighboring spatial unit attribute feature values, and its value ranges from -1 to 1 [37]. When Moran's index is greater than 0, it indicates the existence of positive autocorrelation. Conversely, it indicates negative autocorrelation; the Moran's *I* index is close to 0, which indicates the absence of spatial autocorrelation. Moran's index is calculated by the following formula:

$$
Moran's\ I = \frac{n \sum_{i=1}^{n} \sum_{i=1}^{n} W_{ij} (x_i - \bar{x})(x_j - \bar{x})}{\sum_{i=1}^{n} \sum_{i=1}^{n} W_{ij} (x_i - \bar{x})^2}
\tag{2}
$$

where n is the total number of image elements in the region; x_i and x_j are the values of regions i and j, respectively; $\bar{x}$ is the mean value of variable x. $\sum_{i=1}^{n} \sum_{i=1}^{n} W_{ij}$ is the sample variance; W_{ij} is the weight matrix.

2.4. Data Analysis

Microsoft Excel 2016 and IBM SPSS Statistics 24.0 software were used for statistical analysis. ArcGIS 10.6 software was used for spatial interpolation analysis and mapping. The Moran indices were all calculated using GeoDa 1.18 software (http://geodacenter.github.io, accessed on 18 March 2021).

3. Results and Discussion

3.1. Basic Soil Properties of the Watershed

Soil erodibility can be considerably affected by the inherent soil properties and extrinsic conditions [38,39]. Among them, soil mechanical composition and organic matter content are key inherent parameters for characterizing the K value. As shown in Figure 2, the soil textures in the watershed were mainly silt clay loam and silt clay, with some sandy clay loam, clay loam, sandy loam, and loam. For the mechanical composition of the soils in the watershed (Figure 3), silt and clay were found to be the dominant particles (63.94–85.21%). Their standard deviations range from 8.84 to 18.80%. The paddy soil has the largest content of fine particles, which is 1.33 times higher than that of the purple soil. Sand content in the watershed: purple soil (36.06%) > Fluvo-auic soil (31.19%) > yellow-brown loam (36.34%) > calcareous soil (25.17%) > paddy soil (14.79%). The silt and clay contents of the soil in the watershed were relatively high, which could be beneficial to water retention because of their large surface areas [40,41].
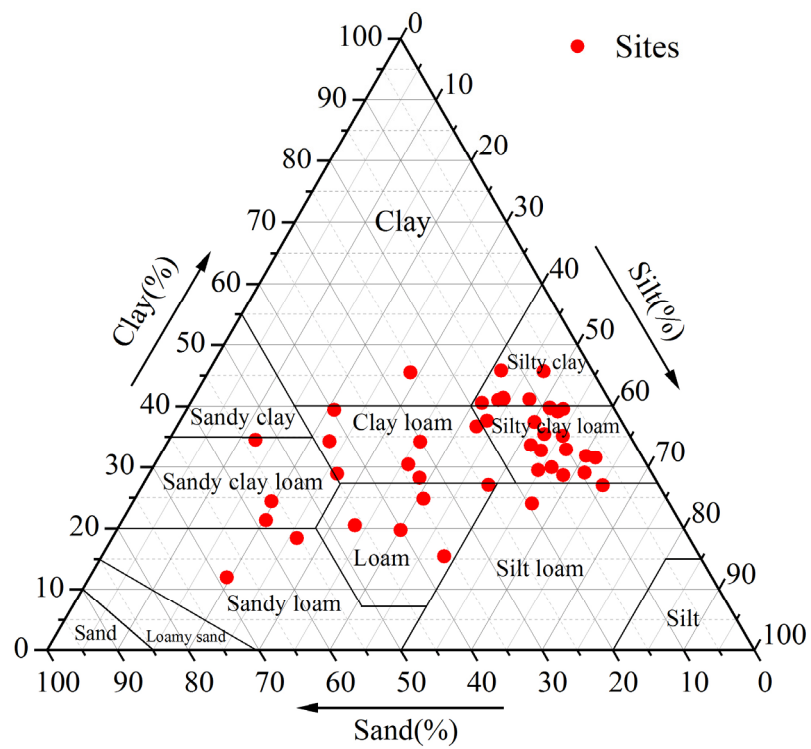
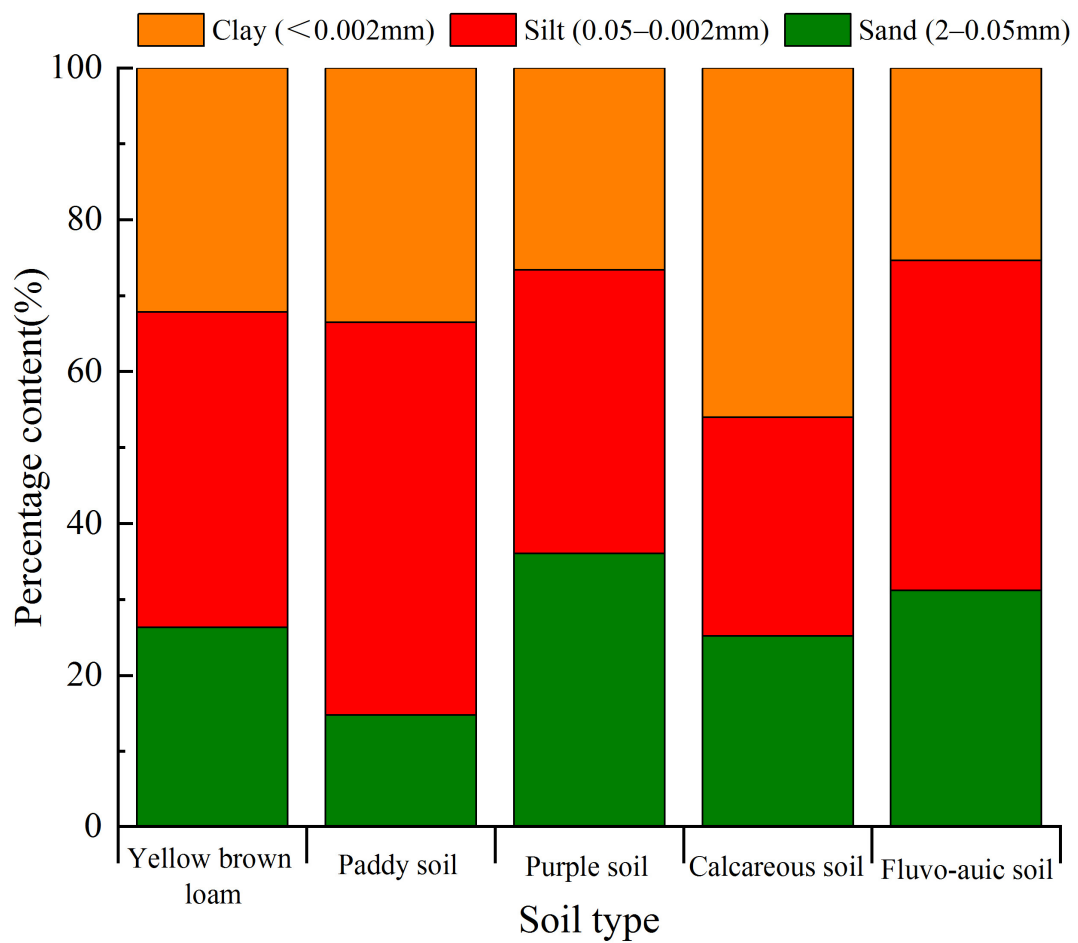**Figure 2.** Soil texture triangle of the sampling sites.

Figure 3. Different soil types of mechanical composition.

The spatial distribution of soil organic matter in the watershed was obtained by ordinary kriging spatial interpolation of soil organic matter content using ArcGIS 10.6 (Figure 4). The variation of soil organic matter in the sub-basin ranged from 3.50 to 39.94 g/kg, with mean and median values of 21.53 and 20.85 g/kg, respectively. The soil organic matter content was generally distributed spatially in a band along the contour direction, with the highest organic matter content in the eastern part of the basin (35.14–39.91 g/kg), gradually decreasing in all directions, and the lowest soil organic matter content in the northeast and southwest. The eastern part of the sub-basin has more rice soils, which is conducive to the accumulation of organic matter on the soil surface.
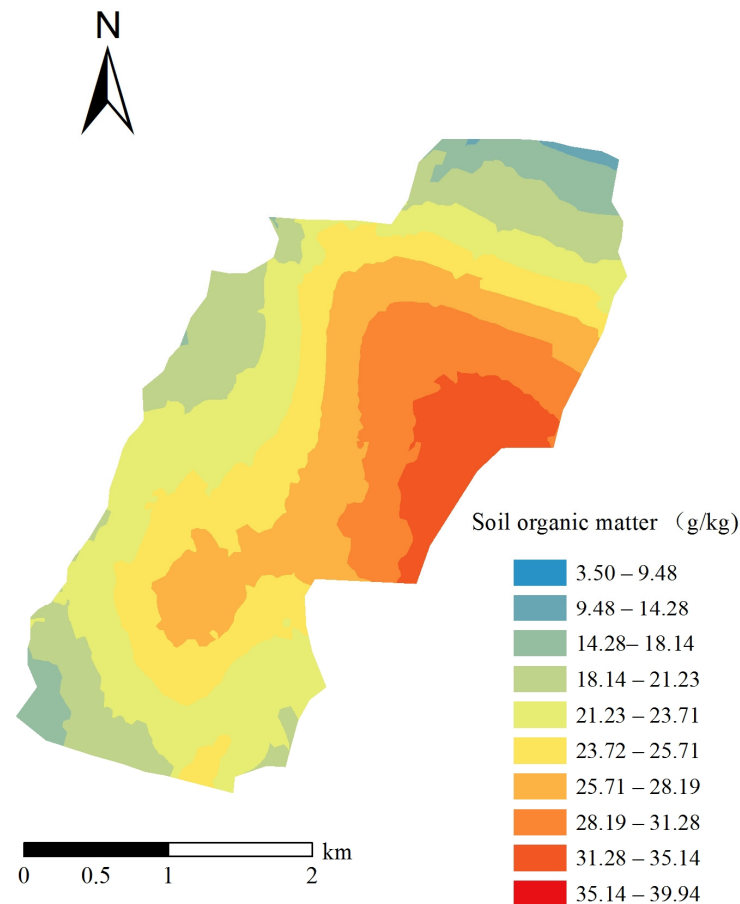

Figure 4. Spatial distribution of soil organic matter in the watershed.

3.2. Soil Erodibility Characteristics of the Watershed

The basic statistics of soil erodibility K values are shown in Table 2. The mean of soil erodibility K values was 0.046 t·hm^2·h/(hm^2·MJ·mm) ranging from 0.039 to 0.052 t·hm^2·h/(hm^2·MJ·mm). The maximum K value was about 1.33 times the minimum value. The variation of the soil erodibility K values in the study area was shown to be small, and the median was close to the mean value, indicating that the distribution of erodibility K values in the watershed were relatively uniform. The coefficient of variation was 18.6%, indicating a moderate degree of variability (CV = 10–20%).

Table 2. Soil erodibility K value statistics (t·hm^2·h/(hm^2·MJ·mm)).

Sampling Points	Max	Min	Median	Mean	SD	Skewness	Kurtosis	CV (%)
46	0.052	0.039	0.047	0.046	0.009	−0.919	−0.186	18.60

Note: Max—maximum; Min—minimum; SD—Standard Deviation; CV—coefficient of variation.

Figure 5 gives the soil erodibility K map of the study area obtained by the kriging interpolation method. The soil erodibility K values in the watershed showed a block-like structure of spatial distribution with an overall trend of being greater in southwest and smaller in northeast. The soil erodibility K values in the southwest were much larger than other areas, indicating that the soils in this area could be more susceptible to erosion. The general topography of the Changyan watershed is deep in the middle and surrounded by steep mountains and hills on the outside (Figure 1). High-elevation regions in the watershed were used as forests for planting pine trees mainly and the surface soil was rarely disturbed by human activities. However, the moderate- and the low-elevation regions were mainly used as agricultural lands for planting maize, citrus, and other crops, and thus the soil was susceptible to erosional processes. Human activities accelerated decomposition and decreased the accumulation of the soil organic matter, and thus weakened soil erosion resistance. Like the findings of Zhang et al. (2008), soil erodibility K values were observed to not only vary with natural parameters (topography, vegetation, rainfall, etc.), but also be affected by the anthropogenic influences [42]. The main factor affecting soil erodibility K values in the northern region, which was generally low in elevation, was the vegetation. Vegetation types, growth years, and above and below ground biomass patterns affect the accumulation of soil organic matter, which results in variable abilities of soil resistance to erosion.
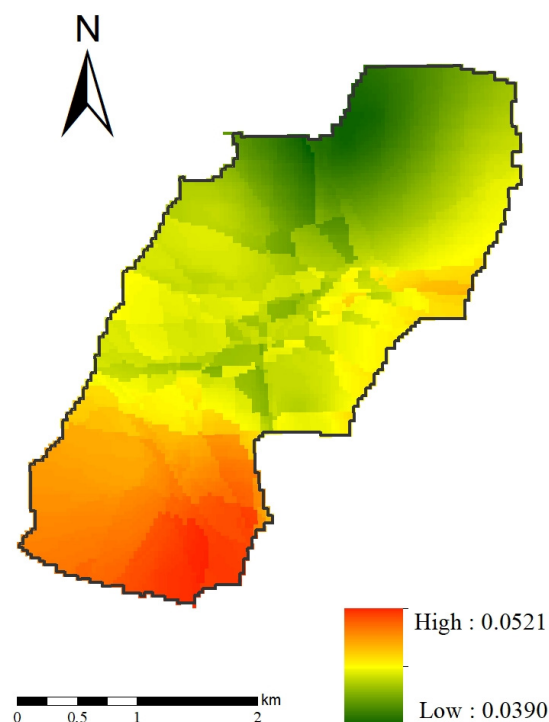

Figure 5. Spatial distribution of soil erodibility K values in the watershed (t·hm^2·h/(hm^2·MJ·mm)).

3.3. Spatial Correlation of Soil Properties in the Watershed

The Moran's I index is a standard measure of autocorrelation used in spatial statistics. For cases with Moran's I index greater than 0, the investigated factors can be considered to be positively correlated. On the other hand, it is negatively correlated. When the absolute value of Moran's I index approaches 1, the spatial correlation will be more significant [43]. We determined the Moran's I index of the soil erodibility (K), mechanical composition, and organic matter content in the study area, which were all positive (see Table 3), and thus they had positive spatial correlations (Z > 1.65, $p < 0.05$). The Moran's I index of the investigated factors ranged from 0.05 to 0.20 following the order of clay content (0.20) > sand content (0.16) > soil organic matter content (0.08) > soil erodibility K value (0.06) > silt content (0.05).

Therefore, the spatial autocorrelation of clay content was the most significant parameter, while the spatial autocorrelation of soil erodibility K value was the least significant one.

Table 3. Moran's I index of basic soil properties and erodibility K values in the study area.

Soil Properties	Moran's I	Z Score	*p*-Value
K (t·hm^2·h/(hm^2·MJ·mm))	0.07	1.88	0.040595
Sand (%)	0.16	3.74	0.000186
Silt (%)	0.05	1.71	0.032018
Clay (%)	0.20	4.46	0.000008
SOM (g/kg)	0.08	2.19	0.028671

Note: K—soil erodibility value; SOM—soil organic content.

4. Discussion

4.1. Relationship between the K Value and Basic Soil Properties

The soils in the study area consist of yellow-brown soil, paddy soil, purple soil, calcareous soil, and fluvo-aquic soil with area ratios of 59.37%, 17.69%, 15.37%, 4.89%, and 2.68%, respectively (Table 4). The soil K values in the watershed varied between 0.0390 and 0.0521 t·hm^2·h/(hm^2·MJ·mm). The calcareous soil had the greatest K value on average, followed by the paddy soil, the yellow-brown soil, the purple soil, and the fluvo-auic soil. The mean K value of calcareous soils was about 1.13 times that of the fluvo-auic soils. This happened because the calcareous soils in the study area were mostly distributed at the upper position of the slopes, which are highly susceptible to physical weathering and chemical dissolution. The purple soils and yellow-brown soils were mainly distributed at the middle and lower position of slopes and were mainly used as forest and orchard for planting Masson's pine, China fir, and citrus. The K values of the five soil types varied within small ranges in the study area with the coefficients of variation changing from 0.92% to 9.79%, which indicated a weak degree of spatial variability. The soil erodibility K values were found significant among the five soil types ($p < 0.05$).

Table 4. Statistics of K values for different soil types (t·hm^2·h/(hm^2·MJ·mm).

Type of Soil	Area (km^2)	Mean	Min	Max	SD	CV (%)
Yellow-brown loam	5.10	0.0453 [a]	0.0390	0.0521	0.0042	9.30
Paddy soil	1.52	0.0458 [b]	0.0405	0.0514	0.0045	9.79
Purple soil	1.32	0.0450 [c]	0.0427	0.0511	0.0034	7.55
Calcareous soil	0.42	0.0498 [d]	0.0490	0.0507	0.0005	0.92
Fluvo-auic soil	0.23	0.0440 [e]	0.0425	0.0456	0.0008	1.86

Note: Different lowercase letters in the same column indicate statistically significant differences among different soil type ($p < 0.05$).

As the soils were initiated from different parent materials, they showed variable mechanical composition and chemical properties. The soil K values also varied with the basic soil properties. Figure 6 showed that the K value had a negative correlation with the soil sand content, while it was positively related to both the soil silt and clay contents. The relationship between the K value and silt content was the most significant one with a linear regression with R^2 = 0.899. Thus, soils containing more silt particles would be more susceptible to erosional processes.

4.2. Relationship between the K Value and Land Use Information

Human activities and vegetation variation due to land use difference result in various effects on the soil properties. Soils covered with a large number of plants generally have a strong microbial activity, which leads to a high organic matter input and decomposition rate. Such soils usually have higher organic carbon contents and large amounts of water-stable aggregates, and thus have a strong ability of resistance to erosion [44]. However, long-term citrus cultivation can lead to unfavorable soil surface conditions, such as soil organic matter

depletion, salt accumulation, and soil compaction [45,46]. As a result, soils with different land use purposes showed various K values (Table 5). The cultivated soils had relatively larger K values, followed by the grassland, the orchard land, and the forest. They all differed significantly ($p < 0.05$). Forest soils were less susceptible to erosion because they were less affected by human disturbance and had higher organic matter content. Besides, soil surface of the forest was covered with organic litters which reduced the energy of the rain splash and surface runoff [47,48]. The results from this study were similar to the findings of Chen et al. (2020) and Zhang et al. (2019) [49,50]. The cultivated, orchard, forest, and grassland soils had a relatively small variability with coefficients of variation ranging from 4.15% to 9.05%.
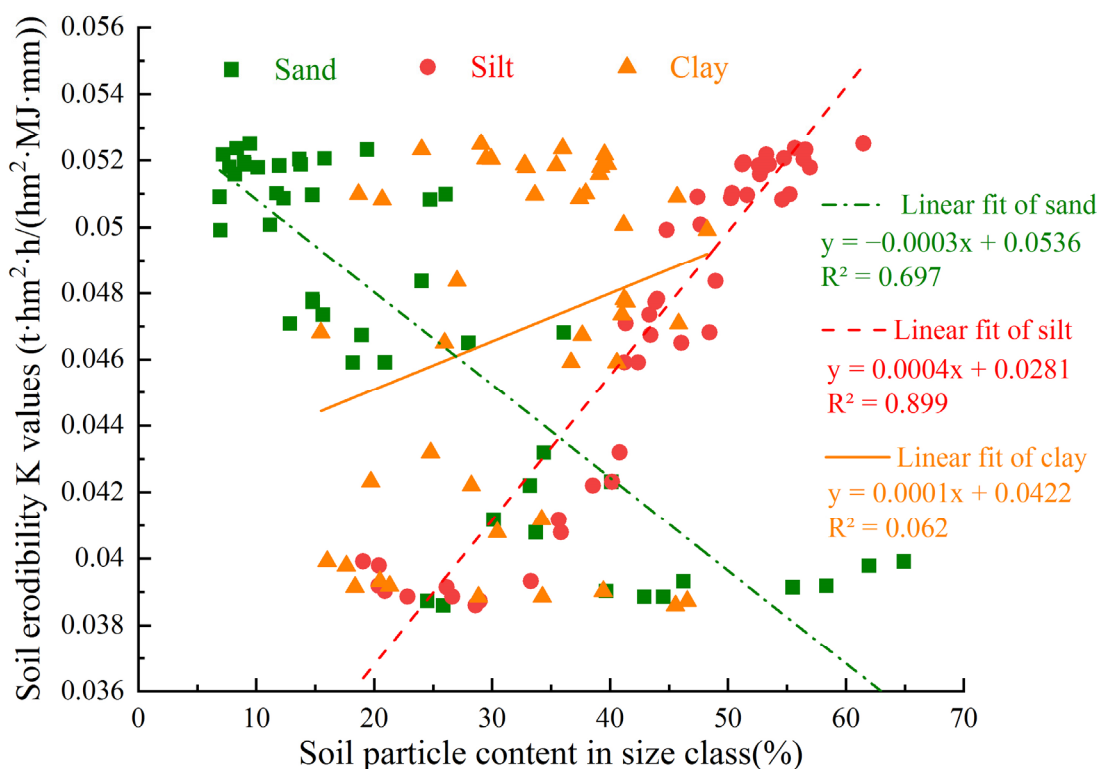

Figure 6. Soil erodibility K values as functions of soil sand, silt, and clay contents.

Table 5. Descriptive statistics of K values for different land use types (t·hm^2·h/(hm^2·MJ·mm)).

Land-Use Type	Max	Min	Median	Mean ± SD	Skewness	Kurtosis	CV (%)
Cultivated land	0.0522	0.0467	0.0504	0.050 ± 0.002 [a]	−0.41	−1.98	4.16
Orchard	0.0507	0.0405	0.0438	0.045 ± 0.003 [b]	0.61	−0.72	6.54
Forest	0.0455	0.0390	0.0422	0.042 ± 0.002 [c]	−0.08	−0.67	4.15
Grassland	0.0516	0.0408	0.0451	0.046 ± 0.004 [d]	0.36	−1.84	9.05

Note: Different lowercase letters in the same column indicate statistically significant differences among different land-use type ($p < 0.05$).

4.3. Relationship between the K Value and Watershed Topography

The topography of the watershed has a significant effect on the thermal and hydraulic conditions of the soils, which has an impact on soil erodibility K values [51]. The Changyan watershed had an elevation ranging from 413 to 919 m (Table 6). Generally, the soil erodibility K values decreased with increasing altitude and showed significant differences ($p < 0.05$). The largest soil K values were observed at positions with an altitude of 413 m. The soils in the lower altitude areas are mainly paddy soils and purple soils used for cultivation. Such soils were usually disturbed by human activities and thus had a weak resistance to erosion. The K values in the areas with altitude greater than 780 m were small,

mostly in the north of the watershed. In such regions, the land was mainly utilized as forest without human activities interfering, and thus had a greater resistance to erosion. On the other hand, as the altitude increased, the vegetation cover increased. Soil organic carbon accumulated more in the higher positions, and thus it resulted in stable soil structures [52].

Table 6. Statistics of K values at different altitudes (t·hm^2·h/(hm^2·MJ·mm)).

Altitude (m)	Max	Min	Median	Mean ± SD	Skewness	Kurtosis	CV (%)
413–420	0.0521	0.0419	0.0511	0.0498 ± 0.003 [a]	−2.14	4.95	6.46
420–486	0.0497	0.0452	0.047	0.0472 ± 0.001 [b]	0.60	0.87	2.5
486–579	0.0488	0.0423	0.0472	0.0467 ± 0.002 [c]	−1.81	4.09	4.13
579–623	0.0504	0.0419	0.0462	0.0463 ± 0.002 [d]	−0.34	0.11	5.25
623–919	0.0514	0.039	0.0459	0.0461 ± 0.004 [e]	−0.54	0.42	8.22

Note: Different lowercase letters in the same column indicate statistically significant differences among different altitude ($p < 0.05$).

Figure 7 gave the correlation between the slope degree and soil erodibility K. Soil erodibility K values in the Changyan watershed were linearly correlated to the slope with a regression of y = 0.0003x + 0.0364 and R^2 = 0.537. Although soil K values varied in small range in the watershed, the trend of soil K value enhanced with increasing slope was significant ($p < 0.05$).
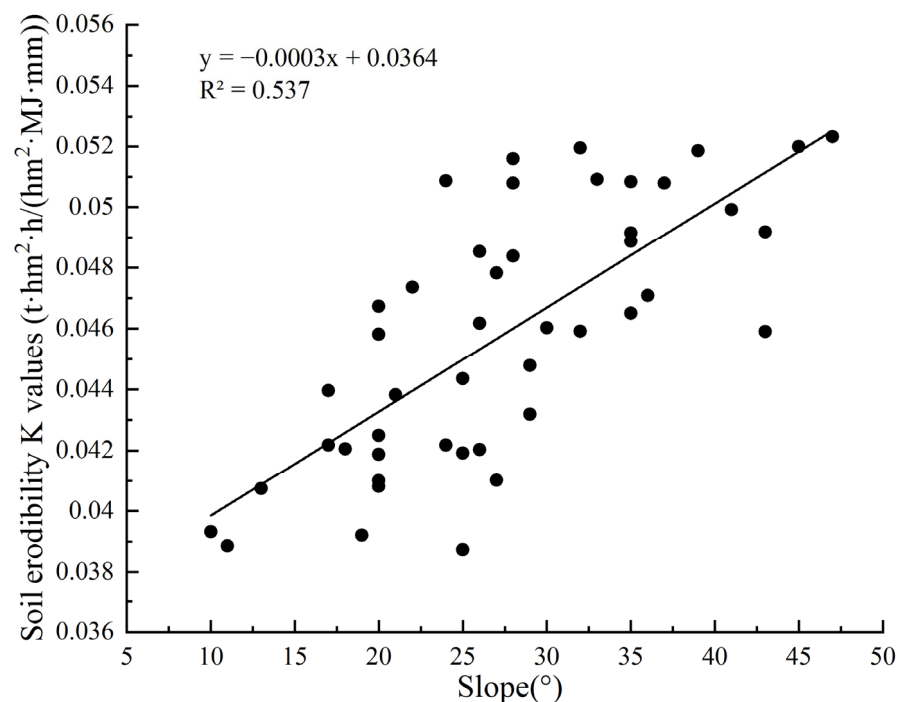

Figure 7. Correlation of soil erodibility K and slope.

5. Conclusions

In this study, we conducted a field survey and GIS interpretation of a watershed in southwest Hubei province of China to evaluate the characteristics of the soil K value and its influencing factors. The main conclusions are:

(1)   The mechanical composition of soils in the Changyan watershed was dominated by silt and clay particles (63.94~85.21%), and the organic matter content was generally increased with decreased altitude. The soil erodibility, mechanical composition, and organic matter content all showed positive spatial autocorrelation in which clay content was the most significant followed by the sand content, the organic matter content, the K value, and the silt content.

(2) The soil erodibility K values in the study area showed a block-like structure of spatial distribution. They were generally greater in the southwest and smaller in the northeast of the watershed. The spatial variability of soil K values for the five soil types in the watershed was relatively small with coefficients of variation ranging from 0.92 to 9.79%.

(3) The soil erodibility K values were spatially related to soil types, land use, and topography. The mean K values of soil for different soil types were ordered as follows: calcareous soil > paddy soil > yellow-brown soil > purple soil > Fluvo-auic soil. The K values were negatively correlated with soil sand content, but positively correlated with soil silt and clay content. Forest soils had the strongest resistance to soil erosion, while cultivated soils had the weakest. Soil erodibility K values enhanced with increasing slope but showed a decreasing trend with increasing altitude.

Author Contributions: X.H.: Methodology, Formal analysis, Writing—original draft. L.L.: Supervision, Funding acquisition. S.D.: Conceptualization. Z.T.: Writing—review and editing. X.Z.: data curation, Investigation. K.W.: Software, Visualization. Y.Z.: Validation. All authors have read and agreed to the published version of the manuscript.

Institutional Review Board Statement: Not applicable.

Informed Consent Statement: Not applicable.

Data Availability Statement: The data presented in this study are available by requesting the author.

Conflicts of Interest: The authors declare no conflict of interest.

References

1. Song, Y.; Liu, L.Y.; Yan, P.; Cao, P. A Review of Soil Erodibility Studies. *Arid. Land Geogr.* **2006**, *29*, 124–131.
2. Huang, Y.H.; Lu, C.L.; Fu, Q.; Shi, Y.Z.; Xu, J.J. Research on Soil Loss Forecasting in Southeast Fujian. *J. Soil Water Conserv.* **1993**, *7*, 13–18.
3. Trimble, S.W.; Crosson, P. LAND USE: U.S. Soil Erosion Rates–Myth and Reality. *Science* **2000**, *289*, 248–250. [CrossRef]
4. Zhang, K.L.; Peng, W.Y.; Yang, H.L. Soil erodibility values and their estimation in China. *Acta Pedol. Sin.* **2007**, *44*, 7–13.
5. Mendona, R.; Müller, R.A.; Clow, D.; Verpoorter, C.; Raymond, P.; Tranvik, L.J.; Sobek, S. Organic carbon burial in global lakes and reservoirs. *Nat. Commun.* **2017**, *8*, 1694. [CrossRef]
6. Wischmeier, W.H.; Mannering, J.V. Relation of Soil Properties to its Erodibility1. *Soil Sci. Soc. Am. J.* **1969**, *33*, 131. [CrossRef]
7. Liu, B.Y.; Zhang, K.L.; Jiao, J.Y. Soil erodibility and its application in erosion forecasting. *J. Nat. Resour.* **1999**, *14*, 345–350.
8. Cao, X.H.; Long, H.Y.; Lei, Q.L.; Zhang, R.L. Assessment and analysis of the top soil erodibility K value in Hebei Province. *Soils.* **2015**, *47*, 1192–1198.
9. Peng, G.; Deng, J.C.; Chai, X.K.; Mu, X.M.; Zhao, G.J.; Shao, H.B.; Sun, W.Y. Dynamic sediment discharge in the Hekou-Longmen region of Yellow River and soil and water conservation implications. *Sci. Total Environ.* **2017**, *578*, 56–66.
10. Jiang, Q.H.; Zhou, P.; Liao, C.; Liu, Y.; Liu, F. Spatial pattern of soil erodibility factor (K) as affected by ecological restoration in a typical degraded watershed of central China. *Sci. Total Environ.* **2020**, *749*, 141609. [CrossRef]
11. Zhang, K.L.; Lian, L.; Zhang, Z.D. Reliability of soil erodibility estimation in areas outside the US: A comparison of erodibility for main agricultural soils in the US and China. *Environ. Earth Sci.* **2016**, *75*, 252. [CrossRef]
12. Wang, H.; Zhang, G.H.; Li, N.N.; Zhang, B.J.; Yang, H.Y. Variation in soil erodibility under five typical land uses in a small watershed on the Loess Plateau, China. *Catena.* **2019**, *174*, 24–35. [CrossRef]
13. Zhang, W.T.; Yu, D.S.; Shi, X.Z.; Zhang, X.Y.; Wang, H.J.; Gu, Z.J. Uncertainty study on prediction of erodibility K values of subtropical soils in China. *Acta Pedol. Sin.* **2009**, *46*, 185–191.
14. Godoi, F.R.; Rodrigues, D.B.; Borrelli, P.; Oliveira, P.T.S. High-resolution soil erodibility map of Brazil. *Sci. Total Environ.* **2021**, *781*, 146673. [CrossRef]
15. Madenoglu, S.; Atalay, F.; Erpul, G. Uncertainty assessment of soil erodibility by direct sequential Gaussian simulation (DSIM) in semiarid land uses. *Soil Tillage Res.* **2020**, *204*, 104731. [CrossRef]

16. Martínez-Murillo, J.F.; Remond, R.; Ruiz-Sinoga, J.D. Validation of RUSLE K factor using aggregate stability in contrasted mediterranean eco-geomorphological landscapes (southern Spain). *Environ. Res.* **2020**, *183*, 109160. [CrossRef]
17. Zhang, Y.; Xu, J.H.; Zeng, G.; Hu, Q. The spatial relationship between regional development potential and resource & environment carrying capacity. *Resour. Sci.* **2009**, *31*, 1328–1334.
18. Xie, H.L. Regional eco-risk analysis based on landscape structure and spatial statistics. *Acta Ecol. Sin.* **2008**, *28*, 5020–5026.
19. Overmars, K.D.; De Koning, G.H.J.; Veldkamp, A. Spatial autocorrelation in multi-scale land use models. *Ecol. Model.* **2003**, *164*, 257–270. [CrossRef]
20. Wang, H.; Liu, X.M.; Zhao, C.Y.; Chang, Y.P.; Liu, Y.T.; Zang, F. Spatial-temporal pattern analysis of landscape ecological risk assessment based on land use/land cover change in Baishuijiang National nature reserve in Gansu Province, China. *Ecol. Indic.* **2021**, *124*, 107454. [CrossRef]
21. Zhao, D.X.; Zhao, X.Y.; Khongnawang, T.; Arshad, M.; Triantafilis, J. A Vis-NIR Spectral Library to Predict Clay in Australian Cotton Growing Soil. *Soil Sci. Soc. Am. J.* **2018**, *82*, 1347–1357. [CrossRef]
22. Zhao, D.X.; Li, N.; Zare, E.; Wang, J.; Triantafilis, J. Mapping cation exchange capacity using a quasi-3d joint inversion of EM38 and EM31 data. *Soil Tillage Res.* **2020**, *200*, 104618. [CrossRef]
23. Ma, G.Y.; Li, J.W.; Fang, Q.Q.; Jiang, H. Soil erosion and available nutrient losses from two typical soils under simulated rainfall conditions. *Chin. J. Ecol.* **2015**, *34*, 2267–2273.
24. Zhang, K.L.; Cai, Y.M.; Liu, B.Y.; Peng, W.Y. Study on the dynamic change pattern of soil erodibility. *Acta Geogr. Sin.* **2001**, *56*, 673.
25. Wang, H.; Zhang, G.H.; Li, N.N.; Zhang, B.J.; Yang, H.Y. Soil erodibility influenced by natural restoration time of abandoned farmland on the Loess Plateau of China. *Geoderma* **2018**, *325*, 18–27. [CrossRef]
26. Panos, P.; Katrin, M.; Cristiano, B.; Pasqualle, B.; Christine, A. Soil erodibility in Europe: A high-resolution dataset based on LUCAS. *Sci. Total Environ.* **2014**, *479*, 189–200.
27. Cai, X.; Zhan, H.G.; Shi, J.B.; Zhang, Y.; Wang, Q.X.; Zhang, X.; Zhao, J.H.; Li, Y.C. Study on the characteristics of soil erosion in the transmission project of South and Central E Zhong. *Trans. Chin. Soc. Agric. Eng.* **2019**, *50*, 57–60.
28. Department of Water Resources of Hubei Province. 2020 Hubei Bulletin of Soil and Water Conservation. Available online: http://slt.hubei.gov.cn/bsfw/cxfw/stbcgb/202110/t20211020_3818824.shtml (accessed on 20 October 2021).
29. Qian, L. Monitoring and Evaluation of Soil and Water Conservation in Hydropower Stations in the Mountainous Region of Southwest China. Master's Thesis, Huazhong Agricultural University, Wuhan, China, 2013.
30. Xu, W.S.; Li, J.F. Research on sustainable land use in the rocky desertification mountainous areas of southwest Hubei. *Sci. Technol. Inf.* **2011**, *252*, 112–113.
31. Zhang, J.L. Valuation of Forest Ecosystem Services in Enshi and Its Spatial and Temporal Variability Analysis. Master's Thesis, Hubei Minzu University, Wuhan, China, 2017.
32. Wu, D.K.; Dai, Y.Q.; Li, S.L.; Han, M. Evaluation of comprehensive benefits of 6 management models for returning farmland to forest in Southwest China. *J. Southwest For. Univ.* **2011**, *31*, 34–38.
33. Cooperative Research Group on Chinese Soil Taxonomy. *Chinese Soil Taxonomy*; Science Press: Beijing, China; New York, NY, USA, 2001.
34. Soil Physics Research Laboratory, Nanjing Institute of Soil Science, Chinese Academy of Sciences. *Soil Physical Property Determination Method*; Science Press: Beijing, China, 1978; pp. 134–137.
35. Bao, S.D. *Soil Agrochemical Analysis*, 3rd ed.; China Agricultural Press: Beijing, China, 2000; pp. 28–29.
36. Williams, J.R.; Renard, K.G.; Dyke, P.T. EPIC: A new method for assessing erosion's effect on soil productivity. *J. Soil Water Conserv.* **1983**, *38*, 381–383.
37. Anselin, L.; Syabri, I.; Kho, Y. GeoDa: An introduction to spatial data analysis. In *Handbook of Applied Spatial Analysis*; Springer: Berlin/Heidelberg, Germany, 2010; pp. 73–89.
38. Wei, H.; Zhao, W.W.; Wang, J. A Review of Soil Erodibility Studies. *Chin. J. Appl. Ecol.* **2017**, *28*, 2749–2759.
39. Hana, H.K.; Viliam, N.; Jirka, S. The effects of rock fragment shapes and positions on modeled hydraulic conductivities of stony soils. *Geoderma* **2016**, *281*, 39–48.
40. Panagopoulos, T.; De Jesus, J.; Blumberg, D.; Ben, A. Spatial Variability of Durum Wheat Yield as Related to Soil Parameters in an Organic Field. *Commun. Soil Sci. Plant Anal.* **2014**, *45*, 2018–2031. [CrossRef]
41. Panagos, P.; Borrelli, P.; Poesen, J.; Ballabio, C.; Lugato, E.; Meusburger, K.; Montanarella, L.; Alewell, C. The new assessment of soil loss by water erosion in Europe. *Environ. Sci. Policy* **2015**, *54*, 438–447. [CrossRef]
42. Zhang, J.C.; Li, H.D.; Lin, J.; Li, Y.J.; Jiang, J.; Tao, B.X.; Zhang, D.M. Spatial variation of soil erodibility K values based on small watershed scale. *Acta Ecol. Sin.* **2008**, *28*, 2199–2206.
43. Wang, G.F.; Zhang, W.P.; Bi, R.T.; Zhang, Q.; Ren, J.; Qiao, L.; Shen, R.Y.; Wang, P.H. Estimation and spatial variability characteristics of deep soil organic matter in farmland at the county scale. *Trans. Chin. Soc. Agric. Eng.* **2019**, *35*, 122–131.
44. Huang, X.Q.; Zhao, Y.J.; Xin, Z.B.; Qin, Y.B.; Yi, Y. Influence of typical land use types on soil physicochemical properties and erodibility in Beijing Mountainous. *Res. Soil Water Conserv.* **2015**, *22*, 5–10.
45. Triantafyllidis, V.; Zotos, A.; Kosma, C.; Kokkotos, E. Environmental Implications from Long-term citrus cultivation and wide use of Cu fungicides in mediterranean soils. *Water Air Soil Pollut.* **2020**, *231*, 218. [CrossRef]
46. Srivastava, A.K.; Singh, S. Citrus Decline: Soil fertility and plant nutrition. *J. Plant Nutr.* **2009**, *32*, 197–245. [CrossRef]

47. Borrelli, P.; Robinson, D.A.; Fleischer, L.R.; Lugato, E.; Ballabio, C.; Alewell, C.; Meusburger, K.; Modugno, S.; Schütt, B.; Ferro, V.; et al. An assessment of the global impact of 21st century land use change on soil erosion. *Nat. Commun.* **2017**, *8*, 1–13. [CrossRef]

48. Xiao, L.; Xue, S.; Liu, G.B.; Zhang, C. Fractal features of soil profiles under different land use patterns on the Loess Plateau, China. *J. Arid. Land.* **2014**, *6*, 550–560. [CrossRef]

49. Chen, Y.; Wei, X.P.; Lei, S. Soil erodibility analysis of different land use types in the Qingmuguan karst trough valley watershed. *Carsol. Sin.* **2020**, *39*, 836–844.

50. Zhang, H.Y.; Wang, K.Q.; Song, Y.L. Soil erosion resistance of different land use types in the Jianshan River Basin, Central Yunnan. *J. Soil Water Conserv.* **2019**, *33*, 50–57.

51. Li, P.; Li, Z.B.; Zheng, Y. Influence of land utilization types on soil erodibility in dry-hot valley in Jinsha River. *Res. Soil Water Conserv.* **2011**, *18*, 16–19.

52. Zhang, Y.Q. Analysis on the vertical differentiation & affected factors of soil erodibility K value in mountain soils of Wuyi Mountain. *Subtrop. Soil Water Conserv.* **2012**, *24*, 19–22.